

UCLA

UCLA Previously Published Works

Title

AFFCK: Adaptive Force-Field-Assisted ab Initio Coalescence Kick Method for Global Minimum Search

Permalink

<https://escholarship.org/uc/item/9176r9pt>

Journal

Journal of Chemical Theory and Computation, 11(5)

ISSN

1549-9618

Authors

Zhai, Huanchen

Ha, Mai-Anh

Alexandrova, Anastassia N

Publication Date

2015-05-12

DOI

10.1021/acs.jctc.5b00065

Peer reviewed

AFFCK: Adaptive Force-Field-Assisted *ab Initio* Coalescence Kick Method for Global Minimum Search

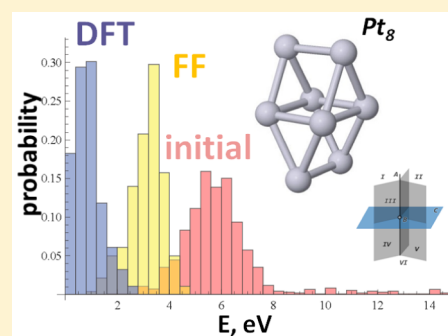
Huanchen Zhai,^{†,§} Mai-Anh Ha,[†] and Anastassia N. Alexandrova^{*,†,‡}

[†]Department of Chemistry and Biochemistry, University of California, Los Angeles, and [‡]California NanoSystems Institute, Los Angeles, California 90095, United States

[§]School of Physics, Shandong University, Jinan 250100, P. R. China

S Supporting Information

ABSTRACT: Global optimization techniques for molecules, solids, and clusters are numerous and can be algorithmically elegant. Yet many of them are time-consuming and prone to getting trapped in local minima. Among the available methods, Coalescence Kick (CK) is attractive: it combines a nearly insulating simplicity with thoroughness. A new version of CK is reported here, called Adaptive Force-Field-Assisted Coalescence Kick (AFFCK). The generation of stationary points on the potential energy surface is tremendously accelerated as compared to that of the earlier, pure *ab initio* CK, through the introduction of an intermediate step where structures are optimized using a classical force field (FF). The FF itself is system-specific, developed on-the-fly within the algorithm. The pre-computed energies resulting from the FF step are found to be surprisingly indicative of energies in subsequent Density Functional Theory optimization, which enables AFFCK to effectively screen thousands of initial CK-generated structures for favorable starting geometries. Additionally, AFFCK incorporates the use of symmetry operations in order to enhance the diversity in the search space, increase the chance for highly symmetric structures to appear, and speed up convergence of optimizations. A structure-recognition routine ensures diversity in the search space by preventing multiple copies of the same starting geometry from being generated and run. The tests show that AFFCK is much faster than traditional *ab initio*-only CK. We applied AFFCK to the search for global and low-energy local minima of gas-phase clusters of boron and platinum. For Pt₈ a new global minimum structure is found, which is significantly lower in energy than previously reported Pt₈ minima. Although AFFCK confirms the global minima of B₅⁻, B₈, and B₉⁻, it proves to be less efficient for systems with nontrivial bonding.



1. INTRODUCTION

Small clusters are of interest in a variety of possible applications, chief among which is catalysis.^{1,2} However, the characterization of small clusters beyond four atoms becomes increasingly difficult with each atomic addition, resulting in a complex potential energy landscape; the global minima of clusters more than four atoms typically have unpredictable geometries with many local minima. Since our intuition for cluster shapes is limited, the search for the experimentally relevant structures—global and thermally accessible low-energy local minima—must be as thorough, automated, and unbiased as possible.

The development of techniques that enable such global optimizations is an established line of research in the scientific community.³ A lengthy appraisal would be due to such methods as the old and robust Monte Carlo (MC) annealing,⁴ the elegant genetic algorithm (GA)-based methods,⁵ the tremendously successful Basin Hopping (BH),⁶ particle swarm,⁷ etc. There are also more modern versions of these: TGMIn is a new version of BH specific to the search for large clusters so that even the characterization of the massive B₄₀ becomes possible at a Density Functional Theory (DFT) level.⁸ Some GAs^{9,10} combine GA with optimization to the local

minima, accelerating the search by employing the knowledge of the gradient on the potential energy surface. Each technique also has caveats. For example, MC is slow and complete sampling is never possible, while GA has a tendency to get stuck in local minima. Hence, faster and more robust methods are desirable. Both the speed of the search and the certainty of the found global minimum structure (especially in the absence of the experimental data to match) need to be improved.

We took arguably the simplest method on the market, called Coalescence Kick (CK) by Averkiev and Boldyrev,¹¹ and advanced it to be significantly faster. CK is based on randomly placing the atoms constituting the cluster in a large Cartesian box, far enough apart, and then pushing them toward the center of mass until they coalesce up to the pairwise sums of known covalent radii. The resultant species is then optimized to the nearest stationary point using an *ab initio* or DFT method. The procedure is repeated *ad nauseum*, and the most stable structure is hypothesized to be the global minimum. The accuracy of the method is high, as was shown in numerous studies where the calculated spectra for the identified global minima were

Received: January 23, 2015

Published: April 15, 2015

symmetry. Hence, we speed up the geometry relaxations for some of these clusters by preparing the symmetric starting structures.

To compensate for this disadvantage and not lose the unbiasedness at the same time, we resort to generating a large number of structures without symmetry, and some structures with all possible symmetry types allowed for a given composition. For each symmetry type, the probabilities for the atoms lying on each special area—such as symmetry elements, their cross positions, and areas divided by the symmetry elements—are equal. Essentially the algorithm requires that the structures generated by the CK method have a particular symmetry. In this process, we put only some of the atoms at random positions in the Cartesian box, whereas the positions of other atoms were calculated by performing symmetry operations. The symmetry is preserved during the coalescence, which then looks like a simple scaling.

Consider the C_{3h} point group symmetry as an example to demonstrate how we can generate random structures with equal probability for atoms lying on each special area. As shown in Figure 2, areas I–VI are equivalent areas, which means that if

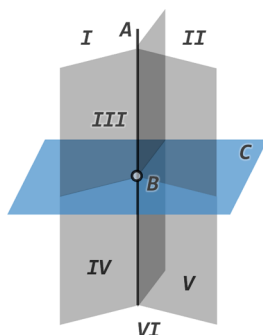


Figure 2. Special areas (I–VI), axis (A), point (B), and plane (C) of a system that has C_{3h} point group symmetry. Atoms located at these positions should be repeated a certain number of times.

we have one atom in area I, we should create five replicas of it in areas II–VI by applying the symmetry operations. So in these areas atoms should be repeated six times. “A” denotes the C_3 rotation axis, where atoms should be repeated two times. “B” denotes the center point, where atoms do not need to be repeated. “C” denotes the mirror plane, where atoms should be repeated three times. Thus, altogether we have four types of special areas.

Given the total number of atoms of one specific atomic type, we should first determine how many atoms will be put in each of these special areas, which forms a combination of integers. If the total number of atoms is not very large, there will be only a few possible combinations. The program will select one of such combinations randomly each time.

If the system is heteroatomic, each atomic type should be treated independently when generating initial symmetry. Currently, all but cubic symmetry point groups (T_d , T , T_h , O_h , I_h) are implemented. The user, however, is responsible for determining which points groups are possible for the given cluster composition, and manually list all or some of them in the input file. The user also has to decide the percentage of structures that should have symmetry (one of the listed ones, chosen at random with equal probabilities); the rest of the population will be generated without symmetry constraints. This method, of course, still leaves a possibility that geometries

generated without symmetry will eventually optimize to symmetric ones, and that symmetric structures would optimize to asymmetric ones. A typical setting that we used for the structures definitely having symmetry was 10–20%.

2.4. Force Field Energy Function. The FF function in the AFFCK method includes three terms (including one constant term),

$$E_{\text{FF}} = \sum_{\text{pairs}} \sum_{\text{types } i} \left(\frac{A_{0i}}{l^9} - \frac{B_{0i}}{l^6} \right) + \sum_{\text{bonds}} (A_1 l^2 + B_1 l + C_1) + E_{\text{const}}$$

where l is the distance between two atoms. The first term denotes the van der Waals (vdW) interaction. We take the 9-6 Lennard-Jones potential for vdW interaction, though more terms for different types of weak interactions could be added. Our first approach was to use the vdW terms for all pairs of atoms not connected by bonds. However, we found that a better fitting result was obtained when vdW interactions were computed for all pairs of atoms, regardless of them being connected by a bond, but depending on how many bonds are formed by the two atom in a pair collectively, vdW parameters are different (fitted independently). For example, in Table 1, we list vdW parameters for pairs of atoms that collectively form fewer than 4 bonds, 4, 5, and 6 bonds, and more than 6 bonds to other atoms, for Pt₈. The second term denotes bond stretching energies. For the first two terms, if the relevant two or three atoms have a different combination of element types, we will use a different set of parameters. Though this is a rather simple FF form, it serves its purpose of a crude preliminary relaxation, as will be shown shortly, and it is very fast to build on-the-fly for every system under consideration. Fine-tuning of FF is not the goal here.

For any structure to be evaluated by the function above, a bond analysis is applied first. We estimate the typical bond length between two atoms by summing their covalent radii, and we accept the maximum bond length by a tolerance value of 0.45 Å, and the minimum bond length is set to be 0.4 Å (data from Jmol¹⁵ settings).

The parameters in the function can be obtained by solving a set of linear equations. Since it is over-determined, it can be solved by the least-squares method. To determine the most suitable number of parameters of each term, we have run several tests for different numbers of parameters. The root-mean-square errors of energies are calculated to indicate which configuration of parameters is better.

The pre-relaxation is done with the Nonlinear Conjugate Gradient method. For the line search part of the CG method, we apply the Newton–Raphson algorithm, which requires the first and second derivatives of the energy function with respect to all coordinates. Since our function is relatively simple, those derivatives are not hard to obtain in analytical forms.

2.5. Details of DFT Calculations. AFFCK may be extended to any DFT package. We have tested it on plane wave DFT software such as the Vienna Ab-initio Simulation Package (VASP)¹⁶ and the Turbomole¹⁷ program to perform DFT calculations. All calculations presented in the paper used the UPBE0¹⁸ hybrid functional, in view of its known adequate performance for both clusters of B¹⁹ and Pt²⁰ and computational affordability. The results for some other exchange correlation functionals may be found in the Supporting Information. The def2-TZVP²¹ basis set was employed. The

Table 1. Fitted Values of Parameters and Corresponding σ_m When Choosing Different Set of Parameters in the Force Field Formula, for Singlet Pt₈ Cluster (PBE0 Functional)^a

no. of parameters	constant term	stretch energy terms	van der Waals interaction terms					σ_m /eV	$\Delta\sigma_m$ /eV
			<4	4	5	6	>6		
3	-954.4	N/A	as (5)	as (5)	151.0 14.01	as (5)	as (5)	0.744	
6	-954.4	0.068 -0.37 0.50	as (5)	as (5)	126.0 12.46	as (5)	as (5)	0.696	0.048
8	-954.3	0.067 -0.36 0.48	as (5)	as (5)	122.5 13.37	as (>6)	123.7 11.59	0.649	0.047
10	-954.3	0.067 -0.36 0.48	as (4)	123.7 13.95	122.7 13.21	as (>6)	123.8 11.56	0.645	0.004
12	-954.3	0.076 -0.41 0.55	68.66 10.96	129.3 14.99	124.7 14.06	as (>6)	127.4 12.6	0.642	0.003
14	-954.2	0.067 -0.36 0.46	132.4 15.9	143.9 16.13	132.2 14.47	134.4 13.59	120.0 10.66	0.593	0.049

^aAll the parameters are calculated using the energy unit hartree and length unit Å. "N/A" denotes that these parameters are not included. The van der Waals interaction terms are divided according to the total number of bonds that the interacting atoms have, and "as (*n*)" denotes that these parameters are taken to be the same as those of the *n* bonds case. $\Delta\sigma_m$ is the difference of σ_m compared to the previous line. The three numbers for each entry in the "stretch energy terms" column are A_1 , B_1 , and C_1 , respectively, and the two numbers for each entry in the "van der Waals interaction terms" columns are A_{0i} and B_{0i} , respectively.

level of theory in use can be adjusted to what is more suitable for the studied systems, and this is one of the levers for increasing the accuracy of the search, if desired. For the purpose of testing AFFCK in this work, UPBE0/def2-TZVP was found to be optimal, providing both reasonable computational time and sampling of CK structures (>96% converged).

Other pure and hybrid exchange correlation functionals were pursued but required greater computational expense and provided a smaller sampling of CK structures (\ll 96% converged) for comparison to AFFCK. These results are presented in the Supporting Information and reflect another important aspect of the search for the global minimum and relevant local minima, i.e., the dependence of binding energies on the program package used, the level of theory pursued, and the exchange correlation function chosen. However, the predominance of certain geometries, whether in Turbomole or VASP, or whether with pure or hybrid functionals, is indicative of both the complexity of the potential energy landscape of these structures and also the relative success we have found in pinpointing important local minima. After the search, the lowest energy structures including the global minimum should be refined at a better level of theory for more accurate ranking. In this work, we report the AFFCK method and the specific clusters (B₈, B₉, and Pt₈) used to test the method. Hence, we do not pursue any further refinement.

3. TEST RESULTS AND DISCUSSION

We illustrate the performance of AFFCK on the Pt₈ cluster. Results for B₉⁻ reproduce earlier findings¹³ and are reported in the Supporting Information.

3.1. The Pt₈ Cluster. The AFFCK method was applied to Pt₈ cluster to find the global minimum and local minima structures under UPBE0/def2-TZVP levels of theory. To illustrate the accuracy and efficiency of AFFCK method, we also perform the pure CK search on the cluster from the same initial guessed structures.

We have done several tests to determine how many parameters we should include in our set for a good FF fitting. The quality of fitting can be evaluated by calculating the root-mean-square error (RMSE) σ_m of the energies:

$$\sigma_m = \sqrt{\frac{\sum_m^k (E_{0k} - E_{FFk})^2}{m}}$$

where m is the total number of initial structures, and E_{0k} and E_{FFk} are energies obtained by Turbomole and fitted FF formula, respectively. The smaller σ_m is, the closer our fitted energies are to the DFT energies. Since the parameters are determined by solving a set of over-determined linear equations, σ_m will always decrease when we increase the number of parameters. The significance of parameters can thus be measured by looking at how much σ_m decreases when we introduce new parameters. The parameter test results are shown in Table 1. From the listed $\Delta\sigma_m$ we can see that we cannot improve the quality of the formula much when splitting vdW terms corresponding to total number of bonds less than or equal to 5. (From 8 parameters to 12 parameters, we have split the vdW interaction terms for "total number of bonds less than or equal to 5" to three independent parts: "less than 4", "equal to 4", and "equal to 5". However, the improvements of the fitting are marginal.)

Table 2. Fitted Values of Parameters, Number of Initial Structures Used in the Force Field Formula, and Corresponding σ_m for Pt_8 Cluster Energies (PBE0 Functional) with Different Spin Multiplicities^a

spin multiplicity	no. of initial structures used	constant term	stretch energy terms	van der Waals interaction terms					σ_m/eV
				<4	4	5	6	>6	
singlet	927	−954.2	0.067	132.4	143.9	132.2	134.4	120.0	0.593
			−0.36	15.90	16.13	14.47	13.59	10.66	
			0.46						
triplet	934	−954.3	0.060	95.85	132.8	130.3	127.9	117.0	0.435
			−0.32	11.86	14.09	13.20	12.16	9.66	
			0.40						
quintet	899	−954.3	0.061	89.22	132.9	130.1	127.5	117.7	0.432
			−0.33	11.47	14.07	13.20	12.16	9.77	
			0.42						

^aNotations and units are the same as in Table 1.

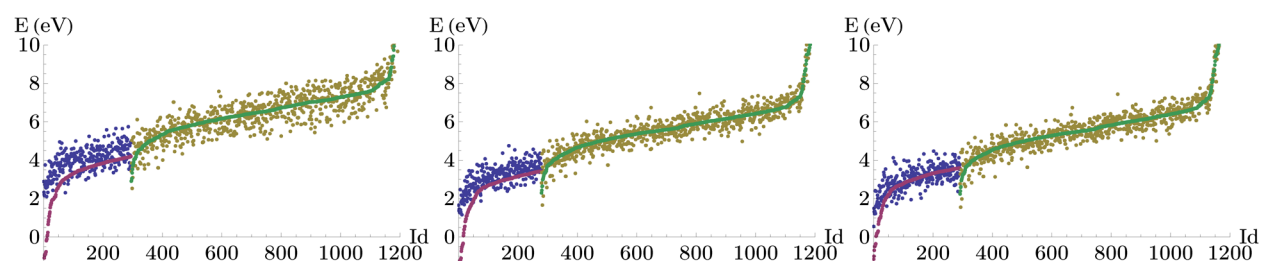


Figure 3. FF and DFT (PBE0 functional) energies of singlet (left), triplet (middle), and quintet (right) Pt_8 clusters. x axes show the serial number of the structures. Green and yellow dots are FF (fitted) and DFT energies of initial structures, respectively; Red and blue dots are FF (predicted) and DFT energies of pre-relaxed structures, respectively. The structures are sorted by their FF energies. Some initial structures with very high energies are excluded in order to show more details of the main part of the plot. Energies relative to $-25\,982.924$ eV, which is the energy of the global minimum that we find, were used.

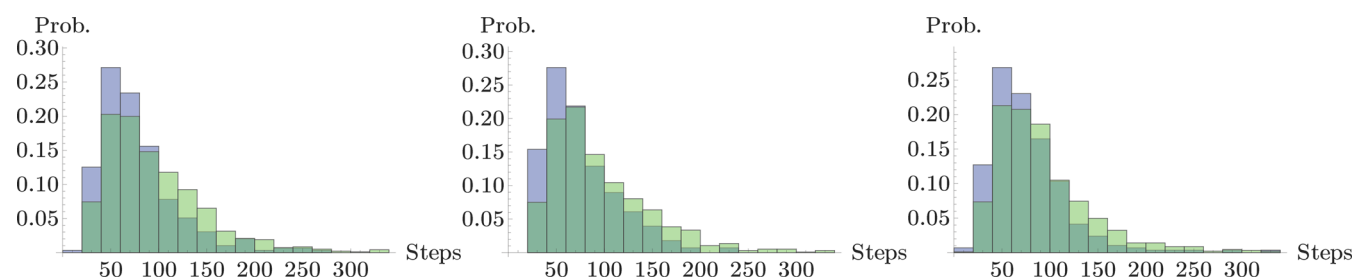


Figure 4. Frequency histograms for the distribution of the number of optimization (DFT with PBE0 functional) steps of converged singlet (left), triplet (middle), and quintet (right) Pt_8 clusters. Blue and green bars are for AFFCK method (optimizing from pre-relaxed structures) and pure CK method (optimizing from initial structures), respectively.

Nevertheless, we choose to keep these parameters since their fitted values are all physical.

To find the accurate global minima for the Pt_8 cluster, we consider different electron spin multiplicities (singlet, triplet, and quintet) independently. This approach was used in both pure CK and AFFCK calculations, which means that, for the AFFCK method, we have different sets of FF parameters fitted for different electronic states. Table 2 lists all these fitted parameters as well as the number of initial structures used for fitting. A total of 1000 initial guess structures for each spin multiplicity were generated, and the DFT single-point energy calculations converged for 956, 963, and 927 structures for singlets, triplets, and quintets, respectively. We chose 97% of them to fit the FF formula, while structures with the top 3% highest energies were excluded.

The fitted FF formula can then be used to find the pre-relaxed structures of the Pt_8 cluster, minima within the FF formalism, as stated in previous sections. For each spin multiplicity, 10 000 additional guessed structures were generated using the CK coalescence approach, without DFT calculations, and pre-relaxed using the Nonlinear CG method and FF. Then, for each spin multiplicity, the selection parameters $d_{\text{rel}} = 0.03$ and $d_{\text{max}} = 0.7$ Å were used to reduce these pre-relaxed structures to the unique set of structures, from which 300 with the lowest FF energies were selected. The selected structures are then re-evaluated and re-optimized using DFT methods.

Now by comparing the approximate FF and DFT energies of these pre-relaxed structures, we can have an idea of the accuracy of AFFCK energies with respect to DFT ones. Figure 3 shows the energies of initial and pre-relaxed Pt_8 clusters, calculated

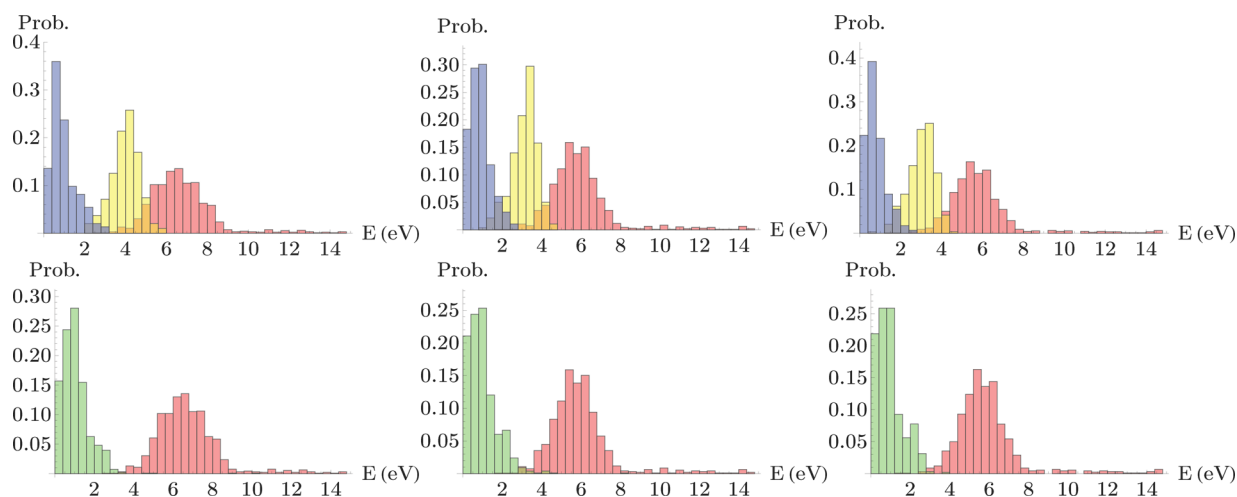


Figure 5. Frequency histograms for energy distributions of singlet (left), triplet (middle), and quintet (right) Pt_8 clusters at different calculation stages. Energy shifts by the AFFCK and pure CK methods are showed in the upper and lower three plots, respectively. All energies are calculated using DFT with the PBE0 functional. Red, yellow, blue, and green parts represent initial, pre-relaxed, DFT relaxed (from pre-relaxed ones), and DFT relaxed (from initial ones) structures, respectively. Energies relative to $-25\,982.924$ eV, which is the energy of the global minimum that we find, were used.

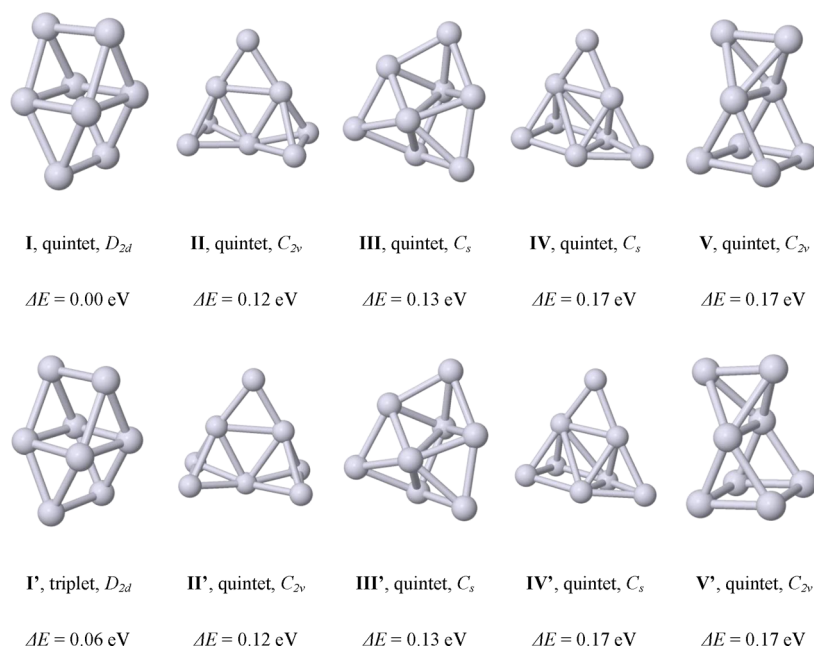


Figure 6. First five local minima of Pt_8 clusters found by the AFFCK (upper) and pure CK (lower) methods. ΔE are energies relative to I, calculated using DFT with the PBE0 functional. For each minimum structure, the spin multiplicity that corresponds to the lowest found energy is listed.

with FF and PBE0, for different spin multiplicities. We can find that the fitting errors for the singlet state are relatively larger than those for the other two states, which agrees with the σ_m values that we have listed in Table 2. Despite this, our simple formula was shown to make a good approximation of DFT energies for Pt_8 clusters, and the fitted parameters obtained from initial structures with high energies did work for structures that have lower energies as well.

The pre-relaxed structures then undergo further optimization by DFT. We can compare the number of steps taken for optimizing pre-relaxed structures (by AFFCK method) and initial structures (by pure CK method) to verify the efficiency of the FF procedure in the AFFCK method. For the pure CK method, the optimizations were converged for 956, 963, and 927 (out of 1000) structures for singlets, triplets, and quintets,

respectively, and for AFFCK method, 295, 279, and 291 (out of 300) structures converged for singlets, triplets, and quintets, respectively. Figure 4 shows the number of steps taken for optimizing these structures with different spin multiplicities. The mean numbers of optimization steps were 96, 97, and 92 (pure CK), and 78, 74, and 76 (AFFCK), for singlet, triplet, and quintet structures, respectively. On average, 20% of the DFT optimization steps were saved per structure, and after considering the number of structures that were used, 76% of the total optimization steps were saved. Additionally, we note that typically AFFCK structures should have more realistic configurations and take less time in one step. From these we can conclude that the AFFCK method indeed accelerated the DFT optimization significantly by the pre-relaxing procedure (which itself is very fast).

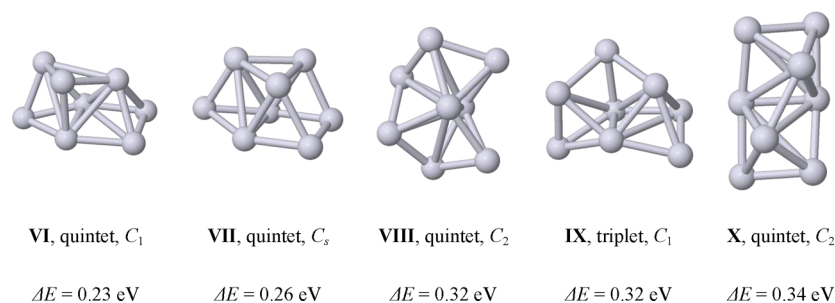


Figure 7. Other higher energy isomers of the global minimum Pt_8 cluster **I** found by AFFCK. ΔE are energies relative to **I**, calculated using DFT with the PBE0 functional. For each structure, the spin multiplicity that corresponds to the lowest found energy is listed.

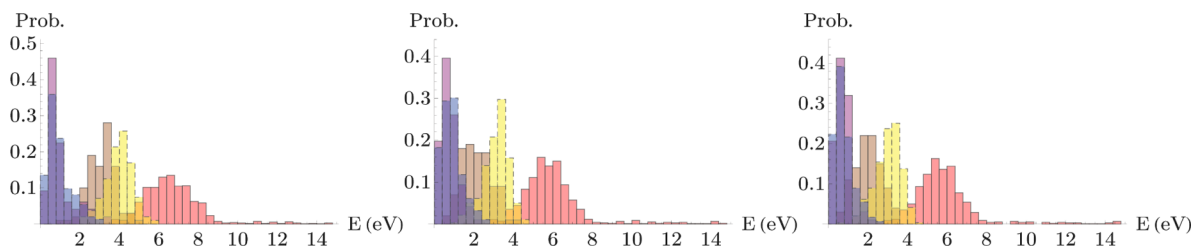


Figure 8. Frequency histograms for energy distributions of singlet (left), triplet (middle), and quintet (right) Pt_8 clusters at different calculation stages. Energy shifts by the normal AFFCK and symmetry-specific AFFCK methods are showed in solid and dashed edges, respectively. All energies are calculated using DFT with the PBE0 functional. Red, yellow, blue, brown, and purple parts represent initial, pre-relaxed (normal AFFCK), DFT relaxed (normal AFFCK), pre-relaxed (SS-AFFCK), and DFT-relaxed (SS-AFFCK) structures, respectively. Energies relative to $-25\,982.924$ eV, which is the energy of the global minimum found by normal AFFCK, were used.

The effectiveness of the pre-relaxing procedure can be further examined by looking at the “energy shift” from initial to final relaxed structures. When energies of the structures to be optimized are closer to those of minima structures, the optimization will be faster. In this case, the “energy shift” will be shorter. Figure 5 shows the energy distribution of Pt_8 structures at different calculation stages. It is obvious that the AFFCK method shortens the “energy shift” by improving the quality of structures initially guessed by the CK method.

In addition to the effectiveness, AFFCK also proves to be accurate for the Pt_8 calculation. The final relaxed structures using the AFFCK and pure CK methods were filtered to find all the unique local minima. The structure selection parameters that we used are $d_{\text{rel}} = 0.015$ and $d_{\text{max}} = 0.2$ Å. Some similar structures were further filtered manually. The first five minima found by each method are shown in Figure 6. Although we optimized much fewer (300) structures in the AFFCK method, the local minimum structures found by the two methods agree with each other. Furthermore, the energy for global minima **I** found by AFFCK is lower than that of **I'** found by pure CK; i.e., with our rather modest CK settings, pure CK failed to find the quintet structure **I**. There is no doubt that increasing the number of trial structures in pure CK would fix the problem. However, notice that in our test roughly 3 times more structures were used in CK versus AFFCK, demonstrating the effectiveness and utility of the FF pre-relaxation. Other local minima that we have found are shown in Figure 7.

3.2. Pt_8 Cluster—Symmetry-Specific Calculation. In the previous section we performed all calculations without any symmetry-specific treatments. Here we further investigate the utility of the symmetry generation procedure, which has been discussed in section 2.3, with the Pt_8 cluster serving as an example. We used the same FF formula as that discussed in section 3.1. Instead of generating 10 000 structures all belonging to the point group C_1 for pre-relaxing, we generated

2100 of those structures with specific point group symmetries, namely, 100 structures for each of C_s , C_i , C_2 , C_3 , C_4 , C_{2v} , C_{3v} , C_{4v} , C_{2h} , C_{3h} , C_{4h} , D_2 , D_3 , D_4 , D_{2h} , D_{3h} , D_{4h} , D_{2d} , D_{3d} , D_{4d} , and S_4 point group symmetry. These 2100 structures were pre-relaxed for different spin multiplicities independently. We then selected 100 structures with lower energies from all unique pre-relaxed structures for DFT optimization for each spin multiplicity (i.e., total of 300, as in the previous situation). We did not specify any particular symmetry requirement in Turbomole so that each structure could also relax to configurations with other symmetries. Figure 8 shows the new energy shifts for this symmetry-specific AFFCK (SS-AFFCK) treatment, with a comparison with the results of AFFCK method without symmetry treatment. We can conclude that the symmetry treatment did not refine the final energy distribution; however, it pushed the pre-relaxed structures closer to the low-energy region. Figure 9 shows a comparison of the number of steps taken in DFT optimization between SS-AFFCK and the normal AFFCK method. We found that the structures treated by SS-AFFCK converged rapidly, with a great increase in the number of structures converging in less than 20 steps. Figure 10 shows some of the relaxed structures found by the SS-AFFCK method. We note that the first three local minima (**I'**, **II'**, and **III'**) have also been found with this treatment. **VIII'** is the mirror-symmetric configuration of **VIII**. **X'** is the same as **X**. Other isomers found here generally have higher energies than those found by normal AFFCK methods, but many of them are of higher order symmetry (especially **XI-T_d** and **XIV-O_h**), and some of them might be saddle points. We also note that **XIV** was reported in previous literatures.¹⁴ Other previously reported Pt_8 structures and their re-optimized energies are listed in the Supporting Information. The isomer **I** that we found is lower in energy than any of those previously reported.

3.3. B_5^- , B_8 , and B_9^- Clusters. Boron clusters recently attracted much attention for their unusual structures, flat or

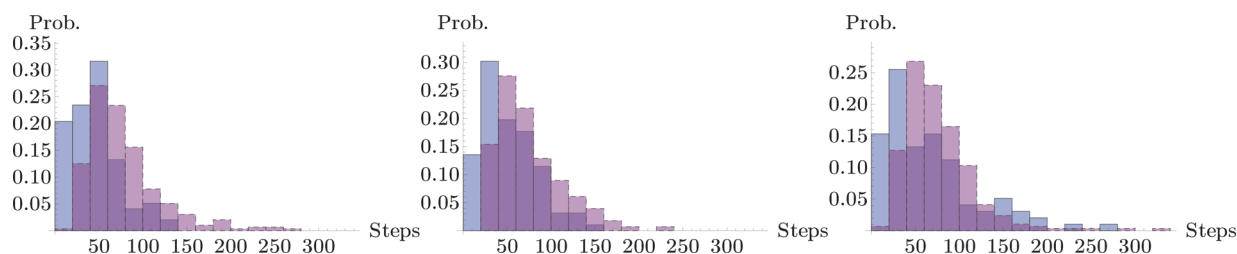


Figure 9. Frequency histograms for the distribution of the number of optimization steps (DFT with PBE0 functional) of converged singlet (left), triplet (middle), and quintet (right) Pt_8 clusters. Blue (solid edge) and purple (dashed edge) bars are for the SS-AFFCK method and the normal AFFCK method, respectively.

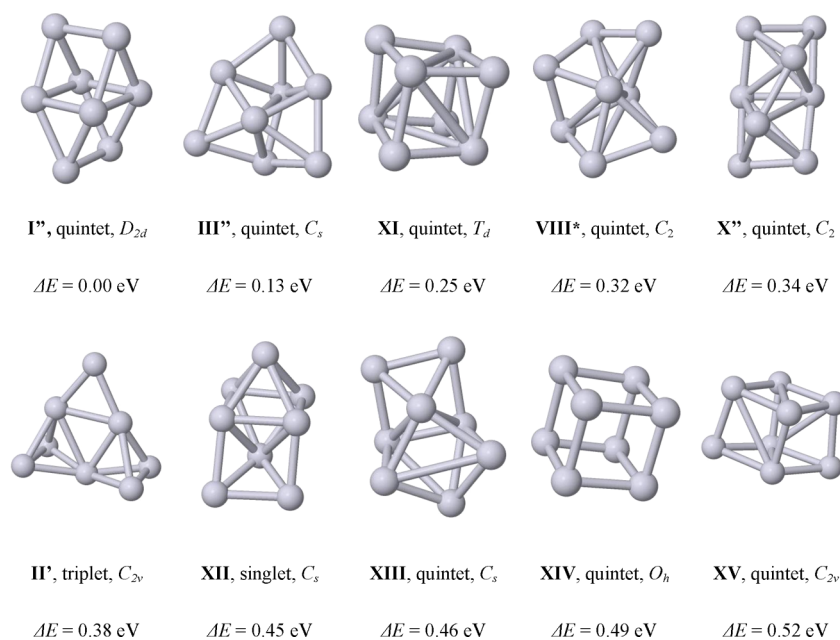


Figure 10. Some representative high-energy isomers of the global minimum Pt_8 cluster I, found by the SS-AFFCK method. ΔE are energies relative to I, calculated using DFT with the PBE0 functional.

nearly flat, as opposed to more globular boranes.^{21,22} The unusual thing about boron clusters is that they are bound by a combination of classical covalent 2c-2e B–B bonds and delocalized σ - and π -bonding, characterizing them as (anti)-aromatic. An additional complication with these systems is that some B atoms (usually found on the periphery of the flat structures) participate in covalent bonding, whereas others found in the middle participate only in delocalized bonding. Hence, B atoms are not all alike in the clusters are instead distinct from one another. As a result, there is a variety of nearly free intra-cluster rotations reported for all-boron systems.^{23,24} Hence, fitting a uniform FF is unlikely to be very successful for these clusters.

We find that the AFFCK method correctly predicts the global minima of B_5^- , B_8 , and B_9^- ;^{13,21,22} however, more initial structures were used in the search. Detailed results for B_9^- are presented in the Supporting Information. Overall, this tells us that AFFCK has its limitations: it is most valuable for clusters that possess no directional covalent bonds but are bound through delocalized bonding. Thus, AFFCK may be the most successful for clusters of main-group metals and transition metals, commonly used in heterogeneous catalysis. We hope our method will be a promising addition to this field. We are currently working on expanding it toward clusters of transition metals deposited on supporting surfaces of semiconductors. For

these systems, the acceleration step should be much appreciated since periodic PAW-DFT calculations are expensive. This extension of the AFFCK method will be a subject of forthcoming publications.

4. CONCLUSIONS

We report a new method, AFFCK, for finding the global and local minima of clusters that outperforms the fastest available method, CK, in terms of speed. Based on traditional CK, AFFCK utilizes an intermediate step in which all candidate structures are pre-computed using a classical FF. Despite the skepticism toward FF in general when applied to clusters, it works surprisingly well as a predictor of relative energies, because FF in AFFCK is learned on-the-fly and specific to every given system under consideration. FF energies of pre-optimized species are shown to be in good agreement with DFT results. The FF generation and pre-relaxation energies are based on linear regression and require little computational cost since they may be calculated on a local computer. The number of steps required for the final DFT geometry optimization of all minima is tremendously reduced and, overall, the method is much more efficient than the traditional CK.

Since AFFCK depends on the first iteration energies of generated CK structures to construct a FF, it will necessarily reflect a potential energy landscape specific to the program

package and level of theory used. Ideally, these potential energy landscapes at high enough theory would reflect the same global minimum and local minima, but under the def2-TZVP level of theory the ranking of Pt₈ minima is dependent on the functional used. We illustrate AFFCK's performance on clusters of platinum and boron. For boron clusters, we confirmed previous predictions. For Pt₈, we identified the global minimum structure and other local minima that are much lower in energy than those previously reported (re-calculated in Turbomole under UPBE0/def2-TZVP level of theory and displayed in the Supporting Information). We also note that for clusters, which possess a mix of covalent and delocalized bonding, such as clusters of boron, AFFCK is less efficient than for all-metal clusters that possess only delocalized bonding. We would recommend AFFCK for clusters of transition metals such as those used in catalysis. We stress that AFFCK proposes a methodology that fine-tunes the breadth of the potential energy landscape pursued, decreases the computational expense, and diversifies the application for users.

■ ASSOCIATED CONTENT

● Supporting Information

Energies of Pt₈ minima calculated using different functionals and of Pt₈ structures found in previous literature, geometries of the global and low-energy local minima of B₉⁻ found by CK and AFFCK, and details illustrating the performance of AFFCK for these B₉⁻ simulations. This material is available free of charge via the Internet at <http://pubs.acs.org>.

■ AUTHOR INFORMATION

Corresponding Author

*E-mail: ana@chem.ucla.edu.

Notes

The authors declare no competing financial interest.

■ ACKNOWLEDGMENTS

We acknowledge support from the NSF CAREER Award CHE1351968 and Air Force Office of Scientific Research under AFOSR BRI Grant FA9550-12-1-0481 to A.N.A., and the CSST Scholarship to H.Z. Computational resources were provided by the UCLA-IDRE cluster.

■ REFERENCES

- (1) Castleman, A. W., Jr; Khanna, S. N. *J. Phys. Chem. C* **2009**, *113*, 2664–2675.
- (2) See, for example: (a) Arenz, M.; Gilb, S.; Heiz, U. In *Atomic Clusters: From Gas Phase to Deposited*; The Chemical Physics of Solid Surfaces 12; Woodruff, D. P., Ed.; Elsevier: Oxford, 2007; pp 1–47. (b) Chrétien, S.; Metiu, H. *Catal. Lett.* **2006**, *107*, 143–147. (c) Heiz, U.; Sanchez, A.; Abbet, S.; Schneider, W.-D. *J. Am. Chem. Soc.* **1999**, *121*, 3214–3217. (d) Haruta, M.; Date, M. *Appl. Catal., A* **2001**, *222*, 427–437. (e) Kaden, W. E.; Wu, T.; Kunkel, W. A.; Anderson, S. L. *Science* **2009**, *326*, 826–829. (f) Lopez, N.; Norskov, J. K. *J. Am. Chem. Soc.* **2002**, *124*, 11262–11263. (g) Molina, L. M.; Hammer, B. *Appl. Catal., A* **2005**, *291*, 21–31. (h) Vajda, S.; Pellin, M. J.; Greeley, J. P.; Marshall, C. L.; Curtiss, L. A.; Balentine, G. A.; Elam, J. W.; Catillon-Mucherie, S.; Redfern, P. C.; Mehmood, F.; Zapol, P. *Nat. Mater.* **2009**, *8*, 213. (i) Yoon, B.; Häkkinen, H.; Landman, U.; Wörz, A. S.; Antoniotti, J.-M.; Abbet, S.; Judai, K.; Heiz, U. *Science* **2005**, *307*, 403–407. (j) Zhang, J.; Alexandrova, A. N. *J. Phys. Chem. Lett.* **2013**, *4*, 2250–2255.
- (3) Wales, D. J.; Scheraga, H. A. *Science* **1999**, *285*, 1368–1372.
- (4) Hammersley, J. M.; Handscomb, D. C. *Monte Carlo Methods*; Methuen: London, 1965.
- (5) (a) Holland, J. H. *Adaptation in natural and artificial systems*; The University of Michigan Press: Ann Arbor, 1975. (b) Deaven, D. M.; Ho, K. M. *Phys. Rev. Lett.* **1995**, *75*, 288.
- (6) Wales, D. J.; Doye, J. P. K. *J. Phys. Chem. A* **1997**, *101*, 5111–5116.
- (7) Call, S. T.; Zubarev, D. Yu.; Boldyrev, A. I. *J. Comput. Chem.* **2007**, *28*, 1177–1186.
- (8) Zhai, H.-J.; Zhao, Y.-F.; Li, W.-L.; Chen, Q.; Bai, H.; Hu, H.-S.; Piazza, Z. A.; Tian, W.-J.; Lu, H.-G.; Wu, Y.-B.; Mu, Y.-W.; Wei, G.-F.; Liu, Z.-P.; Li, J.; Wang, L.-S. *Nat. Chem.* **2014**, *6*, 727–731.
- (9) (a) Alexandrova, A. N. *J. Phys. Chem. A* **2010**, *114*, 12591–12599. (b) Alexandrova, A. N.; Boldyrev, A. I. *J. Chem. Theory Comput.* **2005**, *1*, 566–580.
- (10) Vilhelmsen, L. B.; Hammer, B. *Phys. Rev. Lett.* **2012**, *108*, 126101.
- (11) (a) Averkiev, B. B. Ph.D. Thesis, Utah State University, Logan, UT, 2009. (b) Saunders, M. *J. Comput. Chem.* **2004**, *25*, 621–626.
- (12) (a) Popov, I. A.; Li, W.-L.; Piazza, Z. A.; Boldyrev, A. I.; Wang, A.-L. *J. Phys. Chem. A* **2014**, *118*, 9098–8105. (b) Popov, I. A.; Piazza, Z. A.; Li, W.-L.; Wang, L.-S.; Boldyrev, A. I. *J. Chem. Phys.* **2013**, *139*, 144307. (c) Sergeeva, A. P.; Piazza, Z. A.; Romanescu, C.; Li, W.-L.; Boldyrev, A. I.; Wang, L.-S. *J. Am. Chem. Soc.* **2012**, *134*, 18065–18073.
- (13) Zhai, H.-J.; Alexandrova, A. N.; Wang, L.-S.; Boldyrev, A. I. *Angew. Chem., Int. Ed.* **2003**, *42*, 6004–6008.
- (14) (a) Xiao, L.; Wang, L. *J. Phys. Chem. A* **2004**, *108*, 8605–8614. (b) Nie, A.; Wu, J.; Zhou, C.; Yao, S.; Luo, C.; Forrey, R. C.; Cheng, H. *Int. J. Quant. Chem.* **2007**, *107*, 219–224.
- (15) Jmol: an open-source Java viewer for chemical structures in 3D; <http://www.jmol.org/>. The bond length settings can be found by starting the Jmol program and clicking the “Edit” menu > Preferences > Bonds.
- (16) (a) Kresse, G.; Hafner, J. *Phys. Rev. B* **1993**, *47*, 558–561. (b) Kresse, G.; Hafner, J. *Phys. Rev. B* **1994**, *49*, 14251–14269. (c) Kresse, G.; Hafner, J. *Comput. Mater. Sci.* **1996**, *6*, 15–20. (d) Kresse, G.; Hafner, J. *Phys. Rev. B* **1996**, *54*, 11169–11186.
- (17) *Turbomole*, V6.3 2011, a development of University of Karlsruhe and Forschungszentrum Karlsruhe GmbH, 1989–2007, Turbomole GmbH, since 2007; <http://www.turbomole.com>.
- (18) (a) Perdew, J. P.; Wang, Y. *Phys. Rev. B* **1992**, *45*, 13244–13249. (b) Perdew, J. P.; Burke, K.; Ernzerhof, M. *Phys. Rev. Lett.* **1996**, *77*, 3865–3868. (c) Perdew, J. P.; Ernzerhof, M.; Burke, K. *J. Chem. Phys.* **1996**, *105*, 9982–9985.
- (19) Alexandrova, A. N.; Boldyrev, A. I.; Zhai, H.-J.; Wang, L.-S. *Coord. Chem. Rev.* **2006**, *250*, 2811–2866.
- (20) (a) Shen, L.; Dadras, J.; Alexandrova, A. N. *Phys. Chem. Chem. Phys.* **2014**, *16*, 26436–26442. (b) Ha, M.-A.; Dadras, J.; Alexandrova, A. N. *ACS Catal.* **2014**, *4*, 3570–3580.
- (21) Weigend, F. *Phys. Chem. Chem. Phys.* **2006**, *8*, 1057.
- (22) Alexandrova, A. N.; Zhai, H.-J.; Wang, L.-S.; Boldyrev, A. I. *Coord. Chem. Rev.* **2006**, *250*, 2811–2866.
- (23) Sergeeva, A. P.; Popov, I. A.; Piazza, Z. A.; Li, W.-L.; Romanescu, C.; Wang, L.-S.; Boldyrev, A. I. *Acc. Chem. Res.* **2014**, *47*, 1349–1358.
- (24) Zhang, J.; Sergeeva, A. P.; Sparta, M.; Alexandrova, A. N. *Angew. Chem., Int. Ed.* **2012**, *51*, 8512–8515.
- (25) Martínez-Guajardo, G.; Sergeeva, A. P.; Boldyrev, A. I.; Heine, T.; Ugalde, J. M.; Merino, G. *Chem. Commun.* **2011**, *47*, 6242–6244.